Nonlinear Energy Cascading in Turbulence during the Internal Reconnection Event at the Sino-United Spherical Tokamak *

Song Chai(柴松)[1**], Yu-Hong Xu(许宇鸿)[2], Zhe Gao(高喆)[1], Wen-Hao Wang(王文浩)[1], Yang-Qing Liu(刘阳青)[1], Yi Tan(谭熠)[1]

[1]*Department of Engineering Physics, Tsinghua University, Beijing 100084*
[2]*Southwestern Institute of Physics, Chengdu 610041*

(Received 1 November 2016)

The characteristics of the energy transfer and nonlinear coupling among edge electromagnetic turbulence in thermal quench sub-period of the internal reconnection event (IRE) are studied at the sino-united spherical tokamak device using multiple Langmuir and magnetic probe arrays. The wavelet bispectral analysis and the modified Kim method are applied to investigate linear growth/damping and nonlinear energy transfer rates, along with multi-field turbulence interactions. The results show a multi-field nonlinear energy transfer from electrostatic to magnetic turbulence that results in two-mode coupling in magnetic turbulence, which may play a crucial role to trigger the IRE.

PACS: *52.35.Mw*, *52.35.Ra*, *52.35.Vd* DOI: 10.1088/0256-307X/34/2/025201

In magnetically confined plasmas, microturbulence is generally believed to cause the anomalous transport losses.[1,2] Therefore, it remains one of the important issues in plasma physics to understand the nature of turbulence as well as the energy transfer between multiple turbulent fields. The internal reconnection event (IRE) has been observed in spherical tokamak experiments[3–6] and has been considered as an energy relaxation phenomenon, although the physical mechanisms of the event have not yet been clarified. In this study, we try to uncover a possibility path to describe the triggering mechanism of IRE through the energy transfer and nonlinear coupling.

Considering the relatively short plasma discharge duration and also the transient intermittent event, we use wavelet bispectral analysis[7] to detect the phase coupling that occurs in fluctuating signals in the sino-united spherical tokamak (SUNIST). We have directly calculated the linear growth rate and the nonlinear energy transfer rate of floating potential fluctuation independently, different from the early approach (the method in Ref. [8]) that forces stationary state of turbulence power. The power transfer among multi-field electrostatic and magnetic turbulence has also been investigated.

SUNIST is a small-sized spherical tokamak[9] with a minor radius $a = 0.23$ m and a major radius $R = 0.3$ m. The typical discharge duration is about 15 ms. Two probe arrays are set in a vacuum vessel for this investigation. Probe-1 consists of four tungsten pins tips making quantitative estimations of the linear growth/damping rate and the nonlinear energy transfer rate of turbulence in radial/poloidal directions. Probe-2 is a combination of magnetic (measuring poloidal magnetic field fluctuations $\tilde{B}_\theta$) and the Langmuir probes for detecting the nonlinear energy coupling among electrostatic and electromagnetic fluctuations. Both the probes are mounted on radially movable (manually) shafts at the equatorial plane.

For short-lived intermittent events during the transient discharge period in the SUNIST, the quadratic interaction among the triplet scales a_1, a_2 and a in the time domain is represented by the wavelet cross-bispectrum,[7]

$$B_{xyz}(a_1, a_2) = \int X(a_1, \tau) Y(a_2, \tau) Z^*(a, \tau) d\tau, \quad (1)$$

where $X(a_1, \tau)$, $Y(a_2, \tau)$ and $Z(a, \tau)$ are the wavelet transform of signals $x(t)$, $y(t)$ and $z(t)$, respectively. The integral is taken over a finite time interval T and the scales obey frequency sum rule $1/a = 1/a_1 + 1/a_2$. The squared wavelet cross-bicoherence is the normalized squared cross-bispectrum

$$[b_{xyz}(a_1, a_2)]^2 = \frac{|B_{xyz}(a_1, a_2)|^2}{[\int |X(a_1, \tau) Y(a_2, \tau)|^2 d\tau][\int |Z(a, \tau)|^2 d\tau]}, \quad (2)$$

which can attain values between 0 and 1. For ease of interpretation, the squared bicoherence $[b_{xyz}(a_1, a_2)]^2$ is usually plotted in the (f_1, f_2) plane rather than the (a_1, a_2) plane, by converting the scale lengths into frequencies $f = 1/a$.

To make quantitative estimations of the linear growth rate γ_k and the energy transfer T_k for electrostatic turbulence, we use the modified Kim method based on Kim's and Ritz's methods[8,10] in this study, despite

*Supported by the National Natural Science Foundation of China under Grant Nos 11261140327, 11325524, 11475102 and 11575057, the Chinese National Fusion Project for ITER under Grant Nos 2013GB112001, 2013GB107001 and 2014GB108000, the Tsinghua University Initiative Scientific Research Program, and the 221 Program.

**Corresponding author. Email: chaisong@sunist.org

© 2017 Chinese Physical Society and IOP Publishing Ltd

its stationary condition. We can finally obtain

$$\gamma_k = \frac{1}{\tau}\frac{(\boldsymbol{A}^*)^{\mathrm{T}}\cdot\boldsymbol{F}^{-1}\cdot\boldsymbol{A} - (\boldsymbol{B}^*)^{\mathrm{T}}\cdot\boldsymbol{F}^{-1}\cdot\boldsymbol{B}}{\langle X_k X_k^*\rangle - (\boldsymbol{A}^*)^{\mathrm{T}}\cdot\boldsymbol{F}^{-1}\cdot\boldsymbol{A}}, \quad (3)$$

$$T_k = \sum_{k_1,k_2,k=k_1+k_2} T_k(k_1,k_2) = \sum_{k_1,k_2,k=k_1+k_2} \mathrm{Re}\Big(\frac{|X_k^* Y_k|}{\tau\langle X_k^* Y_k\rangle}\cdot\boldsymbol{Q}\cdot\boldsymbol{A}\Big), \quad (4)$$

where $X_k = \varphi(k,t)$ and $Y_k = \varphi(k,t+\tau)$ represent the input and output signals, respectively. Considering the change of the spectrum in time (from t to $t+\tau$) a spectrum can be written as $\varphi(k,t) = |\varphi(k,t)|e^{i\Theta(k,t)}$. The matrices $\boldsymbol{A} = \langle X_{k_1} \quad X_{k_2} \quad X_k^* \rangle$, $\boldsymbol{B} = \langle X_{k_1} \quad X_{k_2} \quad Y_k^* \rangle$, $\boldsymbol{F} = \langle X_{k_1'} \quad X_{k_2'} \quad X_{k_1}^* \quad X_{k_2}^* \rangle$ $(k_1+k_2 = k_1'+k_2' = k)$ and $\boldsymbol{Q} = (\boldsymbol{B}^*)^{\mathrm{T}}\cdot\boldsymbol{F}^{-1} - L_k\cdot(\boldsymbol{A}^*)^{\mathrm{T}}\cdot\boldsymbol{F}^{-1}$ are defined in Ref. [8].

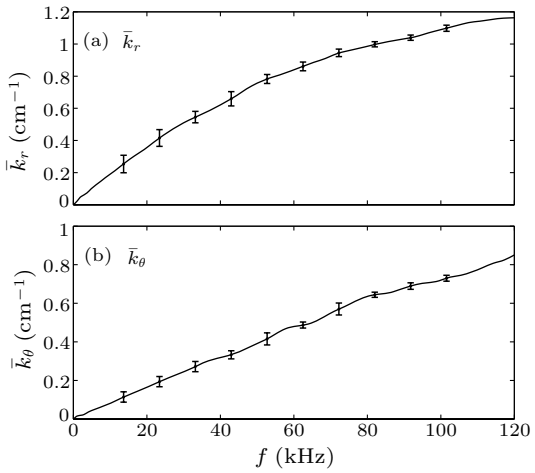

Fig. 1. Statistic dispersion relations of floating potential fluctuations (ϕ_{f}), showing turbulence propagation in (a) radial and (b) poloidal directions around $r-a$=−2 cm.

As pointed out by Ritz *et al.*,[10] we choose the two-point approach to avoid the probe perturbation on plasmas, i.e., measure the time evolution of turbulence at two spatial points (x_1 and x_2) instead of the spatial behavior of turbulence at two times (t and $t+\tau$) with a linear dispersion relation, which is valid in Fig. 1 containing the thermal quench phase before IRE. As can be seen in Fig. 1, the linearity is more pronounced in the poloidal than in the radial direction, implying that, for the two-point approach, the replacement of a temporal growth rate by a spatial one is more reliable by analyzing fluctuation data propagating along the poloidal direction. We first measure the floating potential fluctuations $\varphi(x_1,t)$ and $\varphi(x_2,t)$ from two poloidally (or radially) separated probes located at positions x_1 and x_2 along the wave propagating direction. Then, the wavelet transforms of the input and output signals $\varphi(x_1,t)$ and $\varphi(x_2,t)$ are designated as X_{f} and Y_{f}, respectively. The time delay τ between X_{f} and Y_{f} is estimated from the probe distance ($\Delta x = x_2 - x_1$) and the fluctuation phase velocity (V_{ph}) by $\tau = \Delta x/V_{\mathrm{ph}}$. Finally, based on the above techniques, we can compute the linear growth rate γ_{f} by Eq. (3) and the nonlinear power transfer rate $T_{\mathrm{f}}(f_1,f_2)$ and T_{f} by Eq. (4), respectively.

The IRE is an magnetohydrodynamic (MHD) activity with a property of resiliency specific in the spherical tokamak, which normally evolves for three sub-periods[3–5] (i) thermal quench (TQ), (ii) current increase (CI) and (iii) current quench (CQ), as zoomed in Fig. 2. It is characterized by a positive spike in I_{p} and large bursts in V_{L}, as shown in Figs 2(a) and 2(b). During IRE, the line-averaged density $\overline{n}_{\mathrm{e}}$ decreases and, in the meantime, H_α emission increases abruptly (see Figs 2(c) and 2(d)), indicating a significant particle loss.[3,4] The magnetic fluctuations $\tilde{B}_\theta$ first change slowly in the TQ sub-period then burst quickly in the CI sub-period on a timescale of less than 100 μs (Fig. 2(e)). The frequency spectrum of magnetic fluctuations becomes broadband from the TQ to the CI sub-periods (Figs 2(f) and 2(g)). As simulated in Ref. [12], in this time the micro magnetic turbulence with weak fluctuation power (Fig. 2(f)) and small spatial scale develops to a strong disturbed (Fig. 2(g)) and large spatial scale one. Lastly, it returns to a steady state gradually with a narrow frequency spectrum (Figs 2(h)) during the CQ sub-period.

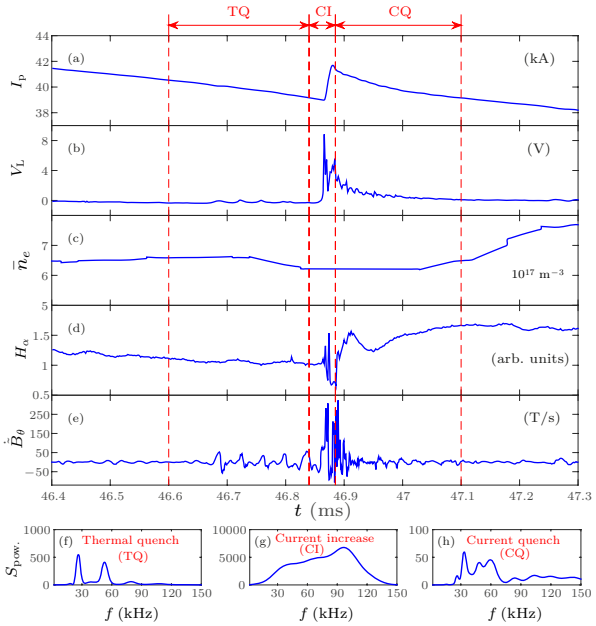

Fig. 2. Time evolutions of (a) plasma current I_{p}, (b) loop voltage V_{L}, (c) line-average density $\overline{n}_{\mathrm{e}}$, (d) radiation H_α and (e) the the differential signal of magnetic fluctuation ($d\tilde{B}_\theta/dt$) during the IRE at the plasma edge ($r-a$=−2 cm). (f)–(h) The frequency spectra of magnetic fluctuation ($S_{\mathrm{pow.}}$) in the TQ, CI and CQ sub-periods, respectively.

To investigate the turbulence interplay during the TQ sub-period, we have analyzed the power spectrum $S(f)$, linear growth rate γ_{f} and nonlinear energy transfer rate $T_{\mathrm{f}}/P_{\mathrm{f}}$ of potential fluctuations $\tilde{\phi}_{\mathrm{f}}$, as shown in

Fig. 3. It has been found that the waves detected by two spatially separated probes along the poloidal and radial directions are different, as can be seen in $S(f)$ of $\tilde{\phi}_{\rm f}$ measured at r_1 or θ_1 (at time t) and r_2 or θ_2 (at time $t+\tau$), respectively. This indicates that large energy losses and wave deformation occur during the wave propagation in the TQ. In both directions, the frequency spectrum $S(f)$ exhibits multiple mode feature (see Figs 3(a) and 3(c)). The low-frequency coherent mode is below 40 kHz, and the high-frequency coherent mode ranges from 50 to 60 kHz. As shown in Figs 3(b) and 3(d), for the low-frequency coherent mode $\gamma_{\rm f} < 0$, i.e., the fluctuation energy arises mainly from the nonlinear coupling whereas for the high-frequency coherent mode the fluctuation energy grows primarily in a linear way ($\gamma_{\rm f} > 0$). The asymmetric $\gamma_{\rm f}$ and $T_{\rm f}/P_{\rm f}$ curves imply possible interaction among multi-field electromagnetic turbulence.

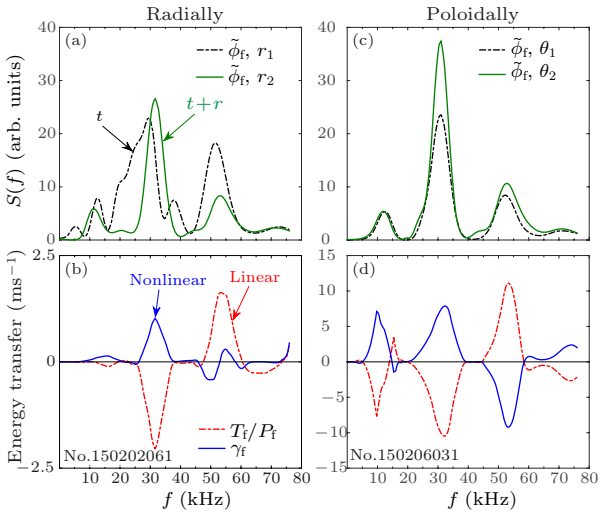

Fig. 3. Power spectrum $S(f)$, linear growth rate $\gamma_{\rm f}$ and nonlinear energy transfer rate $T_{\rm f}/P_{\rm f}$ profiles of $\tilde{\phi}_{\rm f}$ during the TQ sub-period measured by two radially (left column) and poloidally (right column) spaced probes.

Figure 4 illustrates the summed auto- and cross-bicoherence b^2 profiles during the TQ. As is shown, the major fluctuation power in electrostatic turbulence ($\tilde{\phi}_{\rm f}$ and $\tilde{I}_{\rm s}$) is cascaded not only by auto-bicoherence, which is consistent with the nonlinear energy increase in Fig. 3(b), but also by cross-bicoherence with magnetic turbulence ($\tilde{B}_\theta$). In addition, the highest peak from 50 to 60 kHz presents only in the cross-bispectrum $\langle\tilde{\phi}_{\rm f}\tilde{B}_\theta\tilde{B}_\theta^*\rangle$ while for the auto-bispectra of $\langle\tilde{\phi}_{\rm f}\tilde{\phi}_{\rm f}\tilde{\phi}_{\rm f}^*\rangle$ and $\langle\tilde{B}_\theta\tilde{B}_\theta\tilde{B}_\theta^*\rangle$ there is no peak shown in that frequency range. This result suggests a multi-field energy transfer between $\tilde{\phi}_{\rm f}$ and $\tilde{B}_\theta$ fluctuations, which is displayed around (28, 26, 54) kHz in the cross-bispectrum contour plot (Fig. 5(a)). Taking into account the symmetry rules and the fact that f_1 and f_2 are interchangeable, Fig. 5(a) is symmetric with respect to the line $f_1 = f_2$ for $f_2 > 0$ and to the line $f_1 = -f_2$ for $f_2 < 0$. The scale of colors indicates the intensity of the interaction. Hence, the energy power at high frequency in $\tilde{B}_\theta$ cascades nonlinearly from the low frequency component in $\tilde{\phi}_{\rm f}$ or $\tilde{B}_\theta$ fluctuations. This cascading direction can be further verified from the time history of the fluctuation power in Fig. 5(b). During the time period from 46.7 to 46.85 ms in TQ, the fluctuation power in $\tilde{B}_\theta$ at 50–60 kHz gradually increases whereas the fluctuation power of $\tilde{\phi}_{\rm f}$ decreases in 25–30 kHz, revealing the energy transferred nonlinearly from electrostatic to magnetic turbulence.

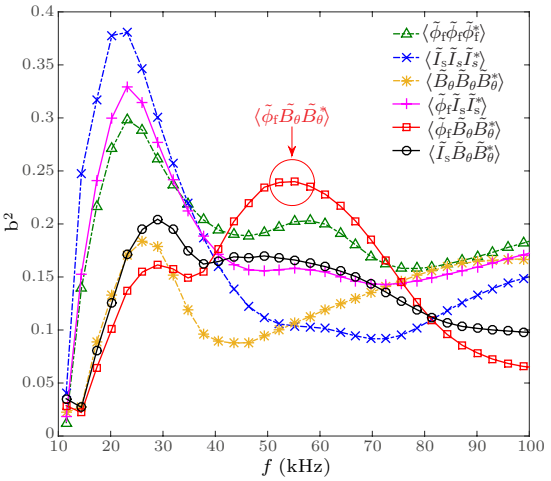

Fig. 4. The total squared auto- and cross-bicoherency b^2 among $\tilde{\phi}_{\rm f}$, $\tilde{I}_{\rm s}$ and $\tilde{B}_\theta$ fluctuations measured during the TQ sub-period (No. 150206031).

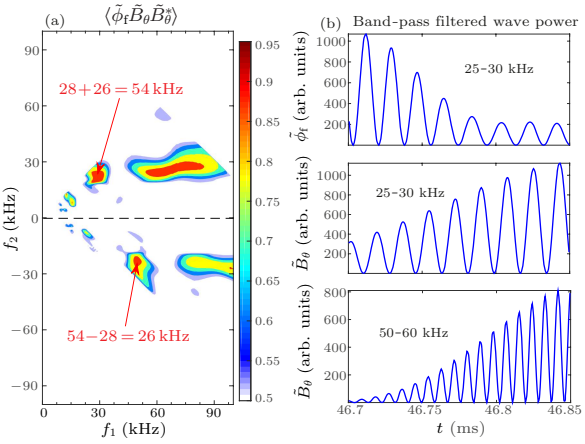

Fig. 5. (a) Contour-plot of the cross-bispectrum $\langle\tilde{\phi}_{\rm f}\tilde{B}_\theta\tilde{B}_\theta^*\rangle$ and (b) time histories of the fluctuation power band-pass filtered in the range of 25–30 kHz for $\tilde{\phi}_{\rm f}$ and $\tilde{B}_\theta$, and in the range of 50–60 kHz for $\tilde{B}_\theta$, respectively, during the TQ sub-period (No. 150206031).

Hayashi *et al.*[11,12] have simulated the magnetic fluctuations during the IRE phase and found that the nonlinear coupling between two magnetic modes, $m/n = 1/1$ and $m/n = 2/2$, in the TQ period may play a crucial role in triggering the IRE. In SUNIST, the magnetic fluctuations in the frequency ranges of 25–30 kHz and 50–60 kHz have been investigated by Liu *et al.*[6] corresponding to $m/n = 3/1$ and m/n=6/2 modes, respectively, in the SUNIST device. Therefore, on the basis of the above computer simu-

lation and experimental measurement the entire physical picture of energy transfer during the TQ might be as follows: at the beginning, the components from low-frequency mode (25–30 kHz) in $\tilde{\phi}_{\rm f}$ and $\tilde{B}_\theta$ are developed independently via the auto-bicoherence or other processes. Then, these two components cross couple each other and transfer energy from $\tilde{\phi}_{\rm f}$ to $\tilde{B}_\theta$, generating a high-frequency mode (from 50 to 60 kHz) in $\tilde{B}_\theta$. After that, the local micro magnetic turbulence accumulates energy and the two low- and high-frequency modes in $\tilde{B}_\theta$ nonlinearly interplay, growing to a large scale with a broad frequency spectrum and strong disturbance,[12] shown in Figs 2(e) and 2(g). Finally, local field lines in torus reconnect, even disrupt, which is the so-called IRE.

After analyses, we could draw the following conclusions. (i) In the TQ sub-period, linear/nonlinear transfer characteristics vary at different frequency ranges. The nonlinear energy coupling dominates in the low-frequency range while the linear transfer dominates in high-frequency range. (ii) The multi-field energy transfer from electrostatic to magnetic fluctuations results in two-mode coupling in magnetic turbulence, growing to a large scale to probably trigger the IRE.

In the future, the multi-field energy cascade in other scenarios, such as in the Mirnov oscillation, current increase and current quench stages, will also be studied. Direct estimates of the energy transfer rates among multi-field turbulence appear to be necessary and the role of linear growth and nonlinear energy transfer should be further evaluated for gaining good plasma confinement.

References

[1] Liewer P C 1985 *Nucl. Fusion* **25** 543
[2] Burrell K H 1997 *Phys. Plasmas* **4** 1499
[3] Sykes A et al 1992 *Nucl. Fusion* **32** 694
[4] Takase Y et al 2001 *Nucl. Fusion* **41** 1543
[5] Sabbagh S A et al 2001 *Nucl. Fusion* **41** 1601
[6] Liu Y Q 2015 Ph. D dissertation: *Study of Magnetohydrodynamic Behaviors during Minor Disruptions in SUNIST Plasmas* (Beijing: Tsinghua University)
[7] Milligen P V, Hidalgo C and Sanchez E 1995 *Phys. Rev. Lett.* **74** 395
[8] Kim J S et al 1996 *Phys. Plasmas* **3** 3998
[9] Peng Y K M and Strickler D J 1986 *Nucl. Fusion* **26** 769
[10] Ritz C P, Powers E J and Bengtson R D 1989 *Phys. Fluids B* **1** 153
[11] Park W B et al 2003 *Nucl. Fusion* **43** 483
[12] Hayashi T, Mizuguchi N and Sato T 2001 *Earth Planets Space* **53** 561